GEOPHYSICAL RESEARCH LETTERS, VOL. 26, NO.5, PAGES 581-584, MARCH 1, 1999

Interhemispheric transport of relativistic electron beams

G. V. Khazanov,[1] M. W. Liemohn,[2] E. N. Krivorutsky,[1] J. U. Kozyra,[2] and B. E. Gilchrist[2]

Abstract. Relativistic electron beam injection simulation results are presented from a new interhemispheric transport model, with a spatial domain reaching from 90 km to 90 km in the conjugate ionospheres. A single beam pulse is injected upward at 700 km during the first time step (10^{-4} s) and allowed to scatter and decay through collisional interactions with neutral particles and the core plasma. The maximum pulse duration for collisional processes to prevail over the wave-beam instabilities is estimated, and the assumed pulse length is well within this limit. For an L=2 field line, the e-folding time of a 5 MeV beam is 265 s, which is much bigger than the bounce period (0.19 s) and comparable to drift period around the Earth.

1. Introduction

In the late 1980s the mildly relativistic (1-10 MeV) electron beam linear accelerators (LINACs) had been reduced in size to the point where they could be feasibly flown onboard spacecrafts, sub-orbital rockets, and balloons. The dynamics of these electron beams injected into the atmosphere from the ionosphere was then studied by *Banks et al.* [1987, 1990]. Neglecting magnetic field effects, it was determined that collisional processes caused significant radial expansion of the beam. *Neubert et al.* [1996] showed, using both Monte Carlo simulations and an analytical description based on the envelope equation [*Humphries*, 1990], that a background magnetic field could significantly reduce beam expansion. Recently, *Habash-Krause* [1998] extended this work to much higher energies (1-100 MeV) and currents (1-10 kA), exploring beam stability issues and a variety of inelastic collision processes to determine bremsstrahlung, X-ray, and optical emission rates. In these studies, however, the authors were focusing only on downward beam propagation from altitudes of 60 km [*Neubert et al.*, 1996] and 350 km [*Habash-Krause,* 1998].

In the work presented here we study a single beam pulse propagation injected upward at 700 km using a Boltzmann kinetic equation model [*Khazanov and Liemohn*, 1995] that has been extended to include relativistic effects. This model allows for study of the time-dependent behavior of the beam flux and its secondaries in the ionosphere-magnetosphere system. For these initial calculations, only the relativistic primary electrons are considered in the model, concentrating on the collisional damping of the beam particles. While wave-particle interactions are often important in relativistic electron transport, this study focuses on the collisional damping of the beam, which is the dominant process when the beam is stable to plasma wave generation.

2. Mathematical formulation

The kinetic equation, which includes the effects of elastic and inelastic collisions with both neutral and charged particles, transport in the inhomogeneous geomagnetic field, and particle sources [*Khazanov and Liemohn,* 1995] can be generalized and adopted for relativistic electrons [*Beliaev and Budker*, 1956; *Hamilton et al.*, 1990; *McTiernan and Petrosian,* 1990],

$$\frac{\varepsilon}{c\sqrt{\varepsilon^2-1}}\frac{\partial\phi}{\partial t}+\mu\frac{\partial\phi}{\partial s}-\frac{1-\mu^2}{2B}\frac{\partial B}{\partial s}\frac{\partial\phi}{\partial\mu}=\frac{AS_E}{10}\frac{\partial}{\partial E}\left[\frac{\varepsilon^2\phi}{E(\varepsilon+1)}\right]+\frac{AS_\mu}{20}\left(\frac{\varepsilon}{E(\varepsilon+1)}\right)^2\frac{\partial}{\partial\mu}\left[\left(1-\mu^2\right)\frac{\partial\phi}{\partial\mu}\right] \quad (1)$$

where $\phi=\phi(t, E, \mu, s)$ is the differential flux of electrons; μ is the pitch angle cosine; E is the electron energy; $\varepsilon=1+E/(mc^2)$; m is the electron mass; s is the coordinate parallel to the geomagnetic field B; c is the speed of light, and $A=2\pi e^4 ln\Lambda=2.6\times10^{-12}$ cm^{2}eV^2. The distribution function of relativistic particles injected in an ionosphere-magnetosphere plasma changes due to Coulomb scattering with thermal electrons and ions, elastic and inelastic interaction with neutral particles and ions, bremsstrahlung and cyclotron radiation [*Petrosian*, 1985]. The input of the two last processes to the evolution of a relativistic beam with a mean energy less than 10 MeV is small and the corresponding terms have been omitted in (1).

The collisional coefficients are contained in the S variables. The term S_E represents the relativistic electron energy loss due to collisions with free electrons, S^E_{ee}; neutrals, S^E_{eN} (per atom); and oxygen ions, $S^E_{eO^+}$. The momentum exchange is presented by the term S_μ and includes the interaction with free electrons, S^m_{ee}; hydrogen and oxygen ions, $S^m_{eH^+}$, $S^m_{eO^+}$; and neutrals, S^m_{eN} (per atom). The expressions for Coulomb scattering and ionization losses are well known [*Rossi and Olbert*, 1970; *Landau and Lifshitz*, 1981] and S_E, S_μ can be presented as:

$$S_E=\sum_{\alpha=e,O^+,N}S^E_{e\alpha}\qquad S_\mu=\sum_{\alpha=e,O^+,H^+,N}S^\mu_{e\alpha} \quad (2)$$

where

$$S^E_{ee}=n_e\ln\left(2\cdot10^{13}\left[\frac{\varepsilon^2-1}{\sum_{\alpha=e,i}n_\alpha/T_\alpha}\right]^{\frac{1}{2}}\right)\qquad S^E_{eO^+}=7\frac{n_{O^+}}{n_e}S^E_{ee}$$

$$S^E_{eN}=\sum_{\alpha=O,N}n_\alpha Z_\alpha\left[\ln\left(1.4\cdot10^{10}\frac{\varepsilon^3}{Z_\alpha^2}\right)-2.9\right] \quad (3a)$$

[1]Geophysical Institute, University of Alaska Fairbanks, AK
[2]Space Physics Research Laboratory, University of Michigan, Ann Arbor, MI

Paper number 1999GL900045.
0094-8276/99/1999GL900045$05.00

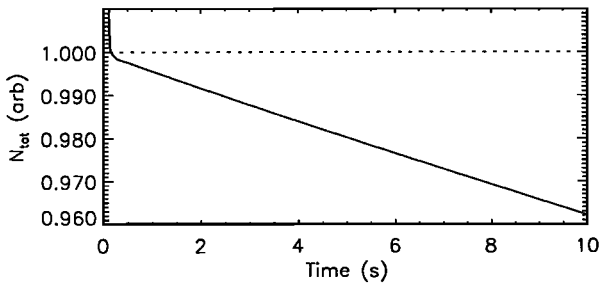

Figure 1. Total beam particle evolution with (solid line) and without (dotted line) collisional interactions.

and

$$S^{\mu}_{ee} = S^{E}_{ee} \qquad S^{\mu}_{eH^+} = \frac{n_{H^+}}{n_e} S^{\mu}_{ee} \qquad S^{\mu}_{eO^+} = \frac{71}{7} S^{E}_{eO^+}$$

$$S^{\mu}_{eN} = \sum_{\alpha=O,N} n_\alpha Z_\alpha (Z_\alpha + 1) \ln\left[140\sqrt{\varepsilon^2 - 1} \Big/ Z_\alpha^{\frac{1}{3}} \right] \tag{3b}$$

Here n_α , T_α and Z_α are the density, temperature, and charge of particles of species α (electrons, ions, and neutral atoms of oxygen and nitrogen). All quantities in (3) are in Gaussian cgs units except energy and temperature, which are in eV.

In order to decrease undesirable computational effects associated with approximation errors of the derivatives $\partial/\partial s$ and $\partial/\partial\mu$, it is convenient to change variables from (s, μ) to (s, μ_0) [*Khazanov et al.*, 1979, 1993], with μ_0 denoting the cosine of the pitch angle at the magnetic equator of the flux tube. This change of variables is desirable because $\phi(s, \mu_0)$ now is a slowly varying function with s (μ_0 is the adiabatic invariant). In this case, (1) becomes

$$\frac{\varepsilon}{c\sqrt{\varepsilon^2-1}} \frac{\partial \phi}{\partial t} + \mu \frac{\partial \phi}{\partial s} = \frac{AS_E}{10} \frac{\partial}{\partial E}\left[\frac{\varepsilon^2 \phi}{E(\varepsilon+1)} \right] + \frac{AS_\mu}{20} \left(\frac{\varepsilon}{E(\varepsilon+1)} \right)^2 \times \left[\frac{(1-\mu^2)(\mu_0^2 - 1 + B_0/B)}{\mu_0^2} \frac{\partial^2 \phi}{\partial \mu_0^2} + \frac{\mu_0^2 - 2\mu_0^4 + 1 - (1+\mu_0^2) B_0/B}{\mu_0} \frac{\partial \phi}{\partial \mu_0} \right] \tag{4}$$

and can be solved numerically as described below, with appropriate initial and boundary conditions [such as those of *Khazanov and Liemohn*, 1995].

Equation (4) is solved with a generalized multi-stream approach taking into account energy degradation, pitch–angle focusing, pitch–angle diffusion, and field-aligned transport. With the following finite-difference approximations,

$$\frac{\partial \phi}{\partial t} = \frac{\phi_n - \phi_{n-1}}{\Delta t}, \quad \frac{\partial \phi}{\partial E} = \frac{\phi_j - \phi_{j+1}}{E_j - E_{j+1}} \tag{5a}$$

$$\frac{\partial \phi}{\partial s} = \begin{cases} \dfrac{\phi_i - \phi_{i-\sigma}}{s_i - s_{i-\sigma}} \end{cases}, \sigma = \frac{\mu_0}{|\mu_0|} \tag{5b}$$

where the subscripts n, i, and j are the time, space, and energy grid step indices, (4) is reduced to

$$A \frac{\partial^2 \phi}{\partial \mu_0^2} + B \frac{\partial \phi}{\partial \mu_0} + C\phi = D \tag{6}$$

Further replacement of μ_0 by $\theta_0 = \cos^{-1}\mu_0$ and the use of

$$\frac{\partial \phi}{\partial \theta_0} = \frac{\delta_1 \phi_{k+1} - (\delta_1 + \delta_2)\phi_k}{\delta_2(\delta_1 + \delta_2)} + \frac{(\delta_1 + \delta_2)\phi_k - \delta_2 \phi_{k-1}}{\delta_1(\delta_1 + \delta_2)}$$

$$\frac{\partial^2 \phi}{\partial \theta_0^2} = \frac{2\delta_1 \phi_{k+1} - 2(\delta_1 + \delta_2)\phi_k + 2\delta_2 \phi_{k-1}}{\delta_1 \delta_2 (\delta_1 + \delta_2)} \tag{7}$$

yields a tridiagonal matrix that is readily solved. In (7), $\delta_1 = \theta_{0,k} - \theta_{0,k-1}$ and $\delta_2 = \theta_{0,k+1} - \theta_{0,k}$. At each energy step, the calculation is swept in both directions along the field line, solving (6) for each hemisphere of flow ($\mu_0 > 0$ and $\mu_0 < 0$), sharing information at the μ=0 boundary and iterating until the energy level has converged at all points in the s-μ_0 plane. More details of this derivation are found in *Khazanov et al.* [1979; 1993] and *Gefan and Khazanov* [1990]. To avoid large numerical diffusion and to obtain second-order accuracy in the time and space steps in (4), the two-step Lax-Wendroff method was used [*Lax and Wendroff*, 1960], which time (space)-centers the integration by defining intermediate values of the dependent variables at the half time (space) steps $t^{n+1/2}$ ($s^{n+1/2}$). After each main step the intermediate values of ϕ are discarded and form no part of the solution [*Potter*, 1973] and thus were omitted in (5) for simplicity.

3. Results

For the results below, the model was run with nine energy steps 0.25 MeV wide each centered at 5 MeV, injected at 700 km at pitch angles between 40° and 90° (equatorial pitch angles of 11.6° to 18.3°). The injection was assumed to be Gaussian with a width of 0.5 MeV. It was run with a time step of 10^{-4} s for an L=2 field line (ionospheric latitude near 45°, with an equatorial plane crossing at 2 R_E geocentric). The spatial domain of the simulation extends from 90 km to 90 km in the conjugate ionospheres, with particles traveling below these altitudes lost to the upper atmosphere. The magnetic field is allowed to vary along s above 200 km, making this altitude the defining point for the loss cone boundary ($\mu_{0,lc}$=16.5°). The injection lasted one time step, and then the beam was allowed to decay with time.

While a standard LINAC has a pulsed beam with an injection lasting several microseconds and a duty cycle around a milli-

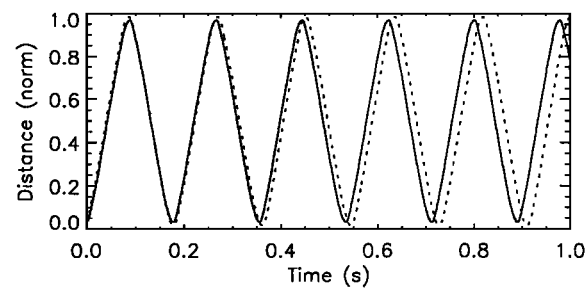

Figure 2. Location of the maximum intensity for 5 MeV at two equatorial pitch angle values, θ_0=18.2° (solid line) θ_0=16.6° (dotted line), for several bounces of the beam. Distance is normalized to the length of the field line (3.5 R_E).

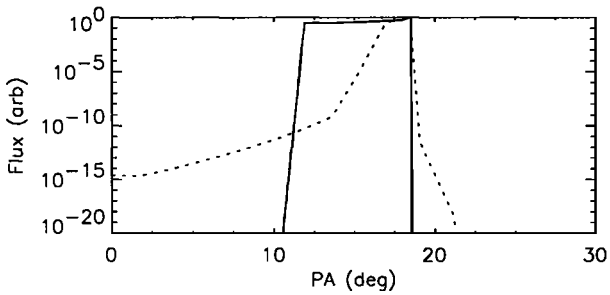

Figure 3. Equatorial pitch angle distributions at 5 MeV for the initially injected profile (solid line) and the quasi-steady-state shape of the distribution after ~10 bounces (dotted line).

second, this simulation is still insightful because the fluxes can be scaled to be the same strength as a single LINAC pulse injection. The results will therefore be presented in normalized units, showing the relative intensity drop of the injection as a function of time and bounce.

Figure 1 shows the evolution the total number of particles in the beam, defined as

$$N_{tot} \propto \int \frac{B_i}{B} ds \int d\mu \int \frac{\phi}{\sqrt{E}} dE \tag{8}$$

The solid line is the simulation with scattering and losses, while the dotted line shows the results from a run with no scattering or loss mechanisms included (except loss to altitudes below 200 km). This means that the dotted line result is a test of the particle conservation due to the spatial derivative. Note that the values are normalized to the steady-state level of the no-loss simulation, and that the y axis is condensed around this value. It is seen that after the initial loss of particles at the end of the first traversal due to the injection pitch angle range spanning part of the loss cone, this line shows no significant loss of particles. The other line shows the effect of scattering on the total number of particles. This curve is expected to have an exponential decline to it from the form of the collision terms, and so an e-folding time for the beam particle count can be calculated as 265 s. Comparing results without either pitch angle scattering or energy loss, it was found that the scattering losses for an injected relativistic electron beam are less than the energy losses. The same tendency was obtained for solar energetic particles [*Petrosian*, 1985].

Shown in Figure 2 is a trace of the beam maximum location as a function of space and time for the first second of simulation, following the max in the 5 MeV intensity for two pitch angles, θ_0=16.6° and 18.2°. The smaller pitch angle magnetically mirrors near 200 km, the boundary of the homogeneous B field regime, and the larger one reflects near the injection altitude of 700 km, so these two curves delimit the portion of the injection that mirrors above the lower boundary (the tapped injection region). It is seen that the bounce period for this beam along an L=2 field line is just about 0.19 s. It is clearly seen in Figure 2 that the bounce period for a particle with fixed energy is a decreasing function of pitch angle.

Equatorial pitch angle distributions are shown in Figure 3. The solid line presents the injected pitch angle distribution. After the first few bounces (10 or so), the solution obtains a distribution (the dotted line) whose time-variation is purely a decrease in magnitude. The larger tail towards smaller pitch angles is due to the larger scattering processes in the thermosphere and ionosphere. Also, in order to negate the effect of the spatial spread of the beam (seen in Figure 2), the fluxes were summed along the flux tube for each μ_0 grid point, which yielded the proper flux for the beam maximum (another test of particle conservation).

4. Discussion and Conclusions

The simulations presented here do not include the effects of plasma waves. This approach is correct if the beam pulse width is below the growth times of the instabilities [*Fisher et al.*, 1988]. The types of excited modes and their evolution depends on the experimental design and processing. Therefore we present below only the estimations of the growth rate for some "hydrodynamic" instabilities (the worse case) to outline approximately the pulse width for which the beam energy and momentum degradation arises mainly due to scattering with the background environment. With the choice of beam current 0.1 A, along with the energy, pulse width, and divergence mentioned above (which are very reasonable for the LINAC experiments), we discuss here the two-stream, ion hose, resistive ion hose, and filamentation instabilities.

The beam plasma density n_b can be estimated using the equilibrium radius approach of *Humphries* [1990]. The corresponding beam radius, r_b, is 10^2-10^3 m, a few times less than the Larmour radius of the beam particles. In our simulation domain n_b varies in the range 10^3-10^5 m^{-3}. For times larger than the period of ambient plasma oscillation and a beam density less than the density of the core plasma, the beam is completely space charge neutralized. The exact degree of the current neutralization is not essential for the beam under consideration here. The two-stream instability growth rate for such a beam density is [*Davidson*, 1990]

$$(\mathrm{Im}\,\omega)_{\max} \approx \frac{4\pi n_0 e^2 c^2}{\varepsilon}\left(\frac{n_b}{n_0}\right)^{1/3} \approx 10^4 s^{-1} \tag{9}$$

For the ion hose instability [*Buchanan*, 1987], the time for wave growth is

$$\tau \approx \frac{3r_b}{c}\left[\frac{17\varepsilon n_b}{I(kA) n_0 mc^2}\right]^{1/2} \approx 10^{-6} - 10^{-5} s \tag{10}$$

where I is the beam current in kiloamps. The growth time for this instability is much less than in the previous case, but it should be noted that this instability "will saturate at a very low level" [*Buchanan*, 1987] and can be ignored here. The expression used above is obtained for an unmagnetized plasma, but the results are of the same order of magnitude for the magnetized case [*O'Brien*, 1988]. The filamentation instabilty arises usually when the beam-plasma system is current neutralized [*Davidson*, 1990]. The threshold condition for this instability, even supposing that complete current neutralization is not satisfied, is

$$1 < \frac{E}{\varepsilon}\sqrt{\frac{\omega_{pb}}{\omega_{cb}}} \approx 10^{-3} \tag{11}$$

and the beam is stable to filamentation. The resistive hose instability is reported to be the most serious macroinstability in a resistive plasma [*Siambis*, 1992]. In our case it should be

checked for low altitudes. *Habash-Krause* [1998] found that the growth time for this altitude is of order 0.1 s. It can be supposed therefore that for a pulse width of order $< 10^{-4}$ s, the main sources of beam degradation are collisional.

The main result of this analysis is that a relativistic electron beam injected upward will, after any initial losses to the lower atmsophere (depending on the injection pitch angles), very slowly dampen (due primarily to energy losses) with a time scale of hundreds of seconds (τ=265 s for the configuration discussed above). The trapped part oscillates between the mirror points and longitudinally drifts with constant L shell. In our case, the drift period is about 600 s and comparable to the beam e-folding time. Due to the low altitude of injection, only a small fraction of the injected particles are trapped with very large pitch angles. As a consequence, the trapped particles spend a relatively long time in the region of high neutral density. That is why a shorter beam lifetime was found here compared to the case when electrons are injected into the inner radiation zone by a nuclear explosion [*Schulz and Lanzerotti*, 1974]. In the latter case, most electrons apparently have an initial equatorial pitch angle between zero and 50°. For the beam under consideration, it is between 12-18°. The difference in the initial conditions makes a comparison between these two cases difficult, but it is reasonable for the beam considered here to have a smaller decay time. In our calculations the atmospheric model was assumed to be longitudinally independent and therefore the drift term in the kinetic equation (1) was omitted, along with electric fields and magnetic disturbances. The role of all these processes in the relativistic beam evolution will be determined by the specific condition of the experiment and can be easily taken into account based on our newly-developed global model [*Khazanov, et al.*, 1998].

As we pointed out in the introduction, the previous studies of relativistic beam injection were focusing only on downward beam propagation from altitudes of 60 km *Neubert et al.* [1996] and 350 km *Habash-Krause* [1998]. The scenario of our simulation is different and addresses the issue of a single beam pulse injected upward at 700 km. Besides, we have used a completely different technique in our study. A propagation of a point-launched relativistic electron beam is studied using a Boltzmann kinetic equation model [*Khazanov and Liemohn*, 1995] that has been extended to include relativistic effects. Nevertheless we did compare the energy losses of relativistic electrons below 350 km predicted from our model with the *Habash-Krause* [1998] calculations and found very good agreement between the two approaches.

Acknowledgments. This work was partially supported by the U.S. Air Force under contract number F19628-K-0004 and by the National Science Foundation under contract ATM-9800830. The authors would like to especially thank Greg Ginet at the Air Force Research Laboratory, Hanscom AFB.

References

Banks, P. M., A. C. Fraser-Smith, B. E. Gilchrist, K. J. Harker, L. R. O. Storey, and P. R. Williamson, New concepts in ionospheric modification, AFGL-TR-88-0133, Air Force Geophysics Laboratory, 1987.

Banks, P. M., B. E. Gilchrist, T. Neubert, N. Meyers, W. J. Raitt, P. R. Williamson, A. C. Fraser-Smith, and S. Sasaki, Charge-2 rocket observations of vehicle charging and charge neutralization, *Adv. Space Res., 10(7)*, 137, 1990.

Beliaev, S. T., and G. I. Budker, Relativistic kinetic equation, *DAN, 107*, 807, 1956.

Buchanan, H. Lee, Electron beam propagation in the ion-focused regime, *Phys. Fluids, 30*, 221, 1987.

Davidson, R. C., *Physics of Nonneutral Plasmas*, Addison-Wesley Publishing Company, New York, 1990.

Fisher, A. S., R. H. Pantell, J. Feinstein, T. L. Deloney, and M. B. Reid, Propagation of a picosecond-duration, relativistic electron beam through hydrogen at atmospheric pressures, *J. Appl. Phys., 64*, 575, 1988.

Gefan, G. D., and G. V. Khazanov, Non-steady-state conditions of filling up the geomagnetic trap with superthermal electrons, *Ann. Geophys., 8*, 519, 1990.

Habash-Krause, L., The relativistic beam-atmosphere interaction, Ph.D. thesis, University of Michigan, 1998.

Humphries, Jr., S., *Charged Particle Beams*, Wiley-Interscience, New York, 1990.

Hamilton, R. J, E. T. Lu, and V. Petrosian, Numerical solution of the time-dependent kinetic equation for electrons in magnetized plasma, *Astrophys. J., 354*, 726, 1990.

Khazanov, G. V., and M. W. Liemohn,. Nonsteady state ionosphere-plasmasphere coupling of superthermal electrons, *J. Geophys. Res., 100*, 9669, 1995.

Khazanov, G. V., M. A. Koen, S. I. Burenkov, A numerical solution to the kinetic equation for photoelectrons taking into accout the free and trapped zones, *Cosmic Res., 17*, 741, 1979.

Khazanov, G. V., M. W. Liemohn, T. I. Gombosi, and A. F. Nagy, Nonsteady-state transport of superthermal electrons in the plasmasphere, *Geophys. Res. Lett., 20*, 2821, 1993.

Khazanov, G. V., M. W. Liemohn, J. U. Kozyra, and T. E. Moore, Global Superthermal Electron Transport: Photoelectron and Plasma Sheet Electron Sources, *J. Geophys. Res., 103*, 23,485, 1998.

Landau, L. D., and E. M. Lifshitz, *Physical kinetics*, Pergamon Press, New York, 1981.

Lax, P. D., and B. Wendroff, Systems of conservation laws, *Comm. Pure Appl. Math., 13*, 217, 1960.

McTiernan, J. M., and V. Petrosian, The behavior of beams of relativistic electrons under the influence of collisions and synchrotron losses, *Astrophys. J., 359*, 524, 1990.

Neubert, T., B. Gilchrist, S. Wilderman, L. Habash, and H. J. Wang, Relativistic electron beam propagation in the earth's atmosphere: modeling results, *Geophys. Res. Lett., 23*, 1009, 1996.

O'Brien, K. J., Theory of ion-hose instability, *J. Appl. Phys., 65*, 9,1988.

Petrosian, V., Directivity of bremsstrahlung radiation from relativistic beams and the gamma rays from solar flares, *Astrophys. J., 299*, 987, 1985.

Potter, D., Computational Physics, *John Wiley & Sons*, New York, 1973.

Rossi, B., and S. Olbert, *Introduction to the Physics of Space*, McGraw-Hill, New York, 1970.

Schulz, M., and L. J. Lanzerotti,, *Particle Diffusion in the Radiation Belts*, Springer-Verlag, New York, 1974.

Siambis, J. G., Relativistic fluid model of the resistive hose instability, *Phys. Fluids B, 4*, 3390, 1992.

G. V. Khazanov and E. N. Krivorutsky, Geophysical Institute, University of Alaska Fairbanks, P. O. Box 757320, Fairbanks, AK 99775-7320.

B. E. Gilchrist, J. U. Kozyra, and M. W. Liemohn, Space Physics Research Laboratory, University of Michigan, 2455 Hayward, Ann Arbor, MI 48109-2143.

(Received October 15, 1998; revised December 1, 1998; accepted January 22, 1999.)